

Ultra-high Energy Air Showers Observed by ANITA-IV

P. W. Gorham,¹ A. Ludwig,² C. Deaconu,² P. Cao,³ P. Allison,⁴ O. Banerjee,⁴ L. Batten,⁵ D. Bhattacharya,⁶ J. J. Beatty,⁴ K. Belov,⁷ W. R. Binns,⁸ V. Bugaev,⁸ C. H. Chen,⁹ P. Chen,⁹ Y. Chen,⁹ J. M. Clem,³ L. Cremonesi,⁵ B. Dailey,⁴ P. F. Dowkontt,⁸ B. D. Fox,¹ J. W. H. Gordon,⁴ C. Hast,¹⁰ B. Hill,¹ S. Y. Hsu,⁹ J. J. Huang,⁹ K. Hughes,⁴ R. Hupe,⁴ M. H. Israel,⁸ T.C. Liu,¹¹ L. Macchiarulo,¹ S. Matsuno,¹ K. McBride,⁴ C. Miki,¹ J. Nam,⁹ C. J. Naudet,⁷ R. J. Nichol,⁵ A. Novikov,^{12,13} E. Oberla,² M. Olmedo,¹ R. Prechelt,¹ S. Prohira,^{4,12} B. F. Rauch,⁸ J. M. Roberts,¹ A. Romero-Wolf,⁷ B. Rotter,¹ J. W. Russell,¹ D. Saltzberg,¹⁴ D. Seckel,³ H. Schoorlemmer,¹⁵ J. Shiao,⁹ S. Stafford,⁴ J. Stockham,¹² M. Stockham,¹² B. Strutt,¹⁴ M. S. Sutherland,² G. S. Varner,¹ A. G. Vieregg,² S. H. Wang,⁹ and S. A. Wissel¹⁶

¹*Dept. of Physics and Astronomy, Univ. of Hawaii, Manoa, HI 96822.*

²*Dept. of Physics, Enrico Fermi Institute, Kavli Institute for Cosmological Physics, Univ. of Chicago, Chicago IL 60637.*

³*Dept. of Physics, Univ. of Delaware, Newark, DE 19716.*

⁴*Dept. of Physics, Center for Cosmology and AstroParticle Physics, Ohio State Univ., Columbus, OH 43210.*

⁵*Dept. of Physics and Astronomy, University College London, London, United Kingdom.*

⁶*Dept. of Mathematics, George Washington University, Washington D.C.*

⁷*Jet Propulsion Laboratory, California Institute of Technology, Pasadena, CA 91109.*

⁸*Dept of Physics & McDonnell Center for the Space Sciences, Washington Univ in St Louis, MO, 63130*

⁹*Dept. of Physics, Grad. Inst. of Astrophys., & Leung Center for Cosmology and Particle Astrophysics, National Taiwan University, Taipei, Taiwan.*

¹⁰*SLAC National Accelerator Laboratory, Menlo Park, CA, 94025.*

¹¹*Dept. of Electrophysics, National Yang-Ming Chiao Tung University, Hsinchu 30010, Taiwan.*

¹²*Dept. of Physics and Astronomy, Univ. of Kansas, Lawrence, KS 66045.*

¹³*National Research Nuclear Univ., Moscow Engineering Physics Inst., Moscow, Russia.*

¹⁴*Dept. of Physics and Astronomy, Univ. of California, Los Angeles, Los Angeles, CA 90095.*

¹⁵*Max-Planck-Institute fur Kernphysik: Heidelberg, Germany.*

¹⁶*Dept. of Physics, Dept. of Astronomy & Astrophysics, Penn State Univ., University Park, PA 16801*

ANITA's fourth long-duration balloon flight in late 2016 detected 29 cosmic-ray (CR)-like events on a background of $0.37^{+0.27}_{-0.17}$ anthropogenic events. CRs are mainly seen in reflection off the Antarctic ice sheets, creating a characteristic phase-inverted waveform polarity. However, four of the below-horizon CR-like events show anomalous non-inverted polarity, a $\sim 3.2\sigma$ fluctuation if due to background. All anomalous events are from locations near the horizon; ANITA-IV observed no steeply-upcoming anomalous events similar to the two such events seen in prior flights.

Antarctic ice has been recognized for many years as an ideal natural dielectric target for the detection of penetrating ultra-high energy particles such as cosmic neutrinos, via radio emission produced by the Askaryan effect, which leads to impulsive, coherent radio Cherenkov emission from particle cascades in dielectric materials [1–3]. The ANtarctic Impulsive Transient Antenna (ANITA) instrument was designed to exploit this effect by continuous broadband monitoring of several million cubic km of ice in the 200–1200 MHz band from the stratosphere during a long-duration balloon flight [4].

During prior flights, ANITA also found that several dozen ultra-high energy (UHE) cosmic ray (CR) events were also detectable from the payload's stratospheric vantage point [5]. Cosmic ray extensive air showers in the geomagnetic field produce 1° -beamed radio impulses via a charge acceleration mechanism tied to the magnetic Lorentz force $\mathbf{F}_L = q\mathbf{v} \times \mathbf{B}_{geo}$ for particle charge q , velocity \mathbf{v} , and geomagnetic field \mathbf{B}_{geo} . In CR air showers this mechanism dominates over the Askaryan effect, leading to signals with strong correlations in polarization to the local geomagnetic field where the shower propagated.

For the fourth flight of ANITA, we pursued two separate analysis paths, one for neutrinos interacting below the ice surface and detected via the Askaryan channel, and one for CR or

CR-like events, detected via the air shower channel. Results of the ANITA-IV analysis for neutrino events via the Askaryan channel are reported in a separate article [6].

ANITA's effective area for normal UHE CR detection is not competitive with other large ground-based CR observatories [8], but its field-of-view from the stratosphere does provide access to geometries that ground-based CR observatories cannot see. CRs that arrive tangential to Earth's surface may interact in the stratosphere, and the extensive air shower and resulting radio emission may be confined completely to the stratosphere, never intersecting with Earth's surface. Such stratospheric events appear to ANITA as CR events with a source location near, but just above the horizon, in a thin band of atmosphere observed at the limb of the Earth. In contrast, the large majority of CRs which arrive on trajectories that do intersect the Earth appear to ANITA in reflection off the relatively radio-smooth surface of the ice. The reflection causes a phase inversion in the CR waveform, providing a clear distinction between these down-going CRs and their stratospheric counterparts.

In each of two prior ANITA flights where CR observations were made, single anomalous CR events were observed at payload arrival angles of -27° [9] and -35° [11] relative to horizontal. The polarity of these events was not phase-

inverted as was the case for all of the other (several dozen) reflected CRs observed in the below-horizon angular region. No natural origin for the non-inverted polarity has yet been confirmed, though several have been suggested [12, 13]. The events had low probability of being background, and high likelihood of CR origin, especially for the unusual event observed by ANITA-III [11].

ANITA-IV was launched on Dec. 2, 2016, reaching a float altitude of about 40 km several hours later, and flew in the Antarctic polar vortex for 28 days until the flight was terminated on Dec. 29, 2016, about 160 km from the South Pole.

In ANITA-IV data, as for ANITA-III, we were initially blind to event polarity for the CR analysis. The blind analysis used to extract the ANITA-IV CR sample followed closely the methods detailed for ANITA-III, and those described for the neutrino analysis [6]. The CR analysis methods included using cross-correlation with a CR waveform template and polarization correlation with the local geomagnetic field.

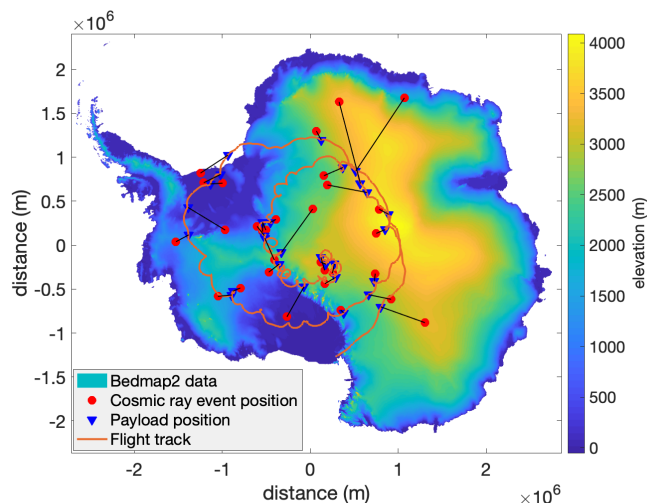


FIG. 1: ANITA-IV flight path and location of payload and apparent event source for each of the 29 events in the final CR sample.

Applying both the template and geomagnetic requirements to events in clusters provides a statistical sideband sample from which to determine the anthropogenic background, which is assumed to “leak” out from clusters into isolated single events, becoming potential background. The final signal analysis is still blind to polarity at this stage, and a detailed analysis of the anthropogenic sample, including estimates of standard errors, gives a background estimate of $0.37^{+0.27}_{-0.17}$ events for events of both polarities in the final CR sample. This estimate is dominated by anthropogenic sources; the thermal radio noise background contribution is negligible, $\sim 5 \times 10^{-7}$ events.

The complete unblinded sample of isolated events showed 29 candidates distributed widely across the continent, as shown in Fig. 1. They are consistent with CRs in their template correlation coefficient and geomagnetic parameters

(Fig. 2). The events were observed from payload arrival angles of -36° to -5.5° with respect to horizontal (the horizon appears at about -6° relative to horizontal from stratospheric altitudes). The two events observed from above the horizon are identified as candidate stratospheric air showers, a class of extensive air showers first observed in radio by ANITA [5].

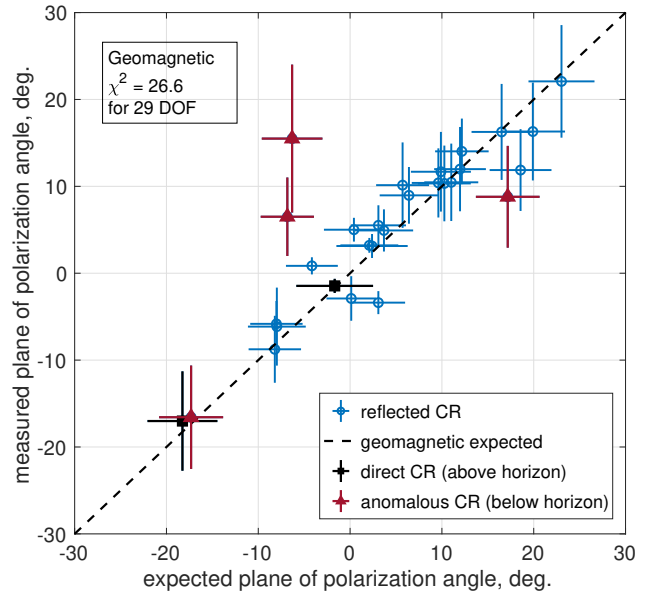


FIG. 2: Geomagnetic correlation of 29 candidate events revealed in our CR analysis.

Prior to determining polarity, the events are processed to form coherently-summed waveforms (CSW). To create these, the individual events from typically 15 different antennas that contain the source within their field-of-regard are combined coherently with group delays that match the source direction, a process also known as beamforming in radio interferometric usage. ANITA’s beamforming typically improves SNR by a factor of three or more compared to the original detection.

ANITA’s CSW show a time-dispersed shape which is caused by the frequency-dependent group delay of different frequency components as they pass through the ANITA antenna, receiver, and digitizer systems. Each intrinsic CR impulse is therefore convolved with this system impulse response, which induces both phase and amplitude distortion in the received signal. This impulse response also varies during the flight, due to changes in the frequency-notch configuration as we work to suppress electromagnetic interference (further details provided in reference [14]).

For accurate estimates of polarity at the best possible SNR, we deconvolve the system impulse response from each waveform. To minimize systematic effects in this process we have utilized four independent methods for deconvolution of the system impulse response:

CLEAN deconvolution is a time-domain method that reconstructs the intrinsic signal using a collection of band-limited δ -function components derived by iterative correlation of the signal with the impulse response function. CLEAN is used extensively for deconvolution of radio interferometric mapping

data [16], but has also been used effectively in time-domain waveform deconvolution [17, 18], and we have found it to be robust for our application (further details provided in reference [14]).

All-pass deconvolution is a Fourier-based partial deconvolution method that sidesteps the difficult problem of division by noisy quantities in the Fourier domain by only removing the phase of system response and leaving the amplitude unchanged. Since ANITA’s system response is dominated by nonlinear phase delays rather than amplitude distortion, this method works well to first order, but can still introduce artifacts due to the lack of amplitude restoration.

Wiener deconvolution performs a complete frequency-domain amplitude and phase correction based on estimates of the signal and noise power spectra [15], but must be carefully applied to avoid accentuating noisy high-frequency components.

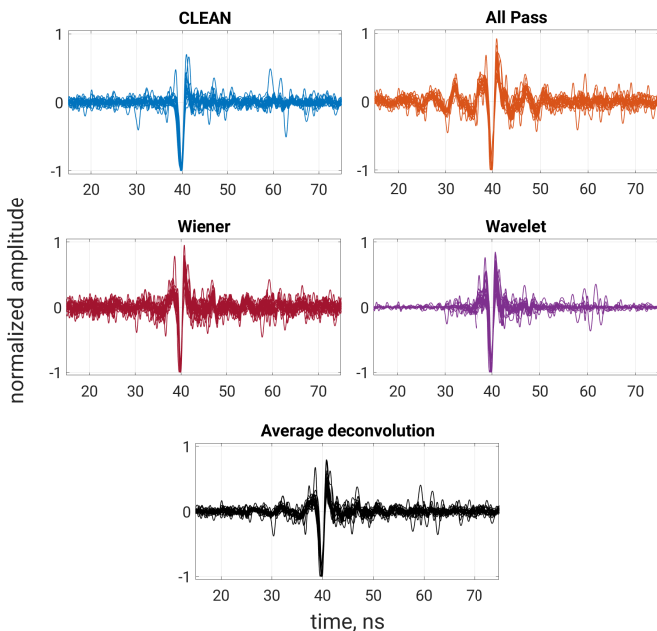


FIG. 3: *Overlays of the 21 normal reflected cosmic ray events in our sample, in each of the four deconvolution methods used, as noted by the title for each pane. The bottom plot gives the average waveform of the four methods.*

Wavelet deconvolution decomposes components of the CSW by projecting it onto a wavelet basis. We employ specific techniques adapted from the FORWARD methodology [19, 20]. Since wavelet bases can be chosen that are naturally commensurate with the impulsive signals that ANITA measures, it is quite effective in both amplitude and phase correction, and in suppressing thermal noise [20].

Calibration errors in portions of the global analysis discovered after the initial CR unblinding required that the data be reanalyzed; this is described in detail in supplementary material [14]. The final subsequent polarity analysis was done after reblinding of the data, including blinding of event number, random event order, and a random polarity factor applied to

all cosmic ray events as the polarity metrics were determined.

Polarity is unrelated to the polarization state of the event; polarity refers to the instantaneous phase of the electric field, whereas polarization refers to the plane of the field oscillation. After deconvolution of the system response, CR events observed by ANITA vary from nearly unipolar, to dominant bipolar, and even include subdominant tripolar events. These effects are believed to be related to the observation angle of the CR relative to the peak of its coherent emission direction. Polarity of a unipolar pulse is simply determined by the single pole. In bipolar events, the order of the two primary poles determines the polarity, and in practice for ANITA data, we find that the sign of leading main pole in a bipolar event determines the polarity. Tripolar components for ANITA events are always subdominant to unipolar or bipolar shapes, and do not affect the polarity determination in general.

After unblinding polarity we find two events have waveforms that produced uncertain estimates of their polarity; coincidentally, both had payload arrival angles of -14.8° . After further investigation, one of these events, 74197411, was found to be adversely affected by high-frequency interference of likely anthropogenic origin. After filtering this interference, the polarity was found to be that of a normal CR. The polarity of the other event, 88992443, could not be resolved, and remains indeterminate for this report. This event has a waveform quite different from all other CR, and has the lowest SNR of any CR observed. Both of these events are excluded from these analyses; their data is provided elsewhere [14].

For the remaining 27 events, the confidence level for polarity determination was found by Monte Carlo methods to be $\sim 99\%$ for one event (19848917), and $\geq 99.99\%$ for the remainder. For 19848917, the $\sim 1\%$ chance of polarity misidentification appears to be due to limitations of our algorithm rather than intrinsic uncertainty in this event’s polarity.

Of the remaining 27 events, 23 events have the normal CR polarity expected from their geometry. Figure 3 shows an overlay of the 21 events with polarity consistent with reflection from the ice sheet surface, the most common type of CR observed by ANITA. Each of the four panes shows the results of the different deconvolution methods described above, along with an overlay of the average of all four waveform methods. This final waveform average was used to determine the polarity in all events.

In addition to the 23 normal reflected CR, four events near the horizon had non-inverted polarity, apparently inconsistent with a reflected CR, though their source locations were determined to be on the ice sheets. Table I shows parameters for the four near-horizon and two above-horizon events. Pointing parameters in these cases used weighted averages of the pointing determined from interferometric maps of both polarizations where there was sufficient SNR. Under the assumption these are CR showers, the table includes estimates of the energy based on scaling from our prior CR energy measurements [8]. The stratospheric events 9734523 and 51293223 are consistent with CRs seen directly as they propagate toward the payload within the stratosphere, at altitude of 18-19 km above the

TABLE I: Preliminary list of stratospheric CR and possible anomalous CR-like events seen by ANITA-IV.

event #	mm dd hh mm ss UTC 2016	Apparent source location Lat.°, Lon.°, alt., m	elev. angle ^a degrees	horizon angle ^a degrees	azimuth degrees	Payload location Lat.°, Lon.°, alt., km	Type ^c	Energy ^d EeV
4098827	12 03 10 03 27	-75.71, 123.99, 3184	-6.17 ± 0.21	-5.92 ± 0.020	337.70	-80.157, 131.210, 38.86	NI	1.5 ± 0.7
9734523	12 05 12 55 40	-71.862, 32.61, 19000 ^b	-5.64 ± 0.20	-5.95 ± 0.020	2.01	-80.9, 31.6, 39.25	AH	...
19848917	12 08 11 44 54	-80.818, -79.87, 758	-6.71 ± 0.20	-6.06 ± 0.020	194.34	-76.66, -72.86, 38.97	NI	0.9 ± 0.5
50549772	12 16 15 03 19	-83.483, 14.73, 2572	-6.73 ± 0.20	-5.92 ± 0.020	234.08	-81.95, 47.29, 38.52	NI	0.8 ± 0.3
51293223	12 16 19 08 08	-74.800, 11.43, 18600 ^b	-5.38 ± 0.24	-5.85 ± 0.020	306.45	-81.7, 39.2, 37.53	AH	...
72164985	12 22 06 28 14	-86.598, 0.35, 2589	-6.12 ± 0.10	-5.93 ± 0.020	140.03	-86.93, -104.29, 38.58	NI	3.9 ± 2.5

^a Both the observed elevation angle of the event, and the apparent horizon here include radio refraction, which lifts the apparent horizon about 0.1° .

^b The source elevation (in the stratosphere) and the given source position are estimates of the approximate location of air shower maximum for these direct stratospheric CR events, determined by using the average column depth to shower max for EeV CRs.

^c AH: above-horizon, direct CR. NI: Non-inverted CR-like event, below horizon.

^d Energy computable for below-horizon events only; above-horizon simulations are beyond our scope in this report. Errors include both statistical and systematic effects.

Earth's surface. As such they enter the Earth's atmosphere at distances beyond the physical horizon, and the resulting particle cascades develop over hundreds of km through the rarefied stratosphere at such altitudes. Estimation of their energies will have to await detailed simulations of these rather extreme form of air showers. These two above-horizon events appear at angles of 0.3° and 0.47° above the horizon, respectively. In other flights we have observed one other stratospheric event at $\sim 0.4^\circ$ above the horizon, and several at larger angles, but none closer than this.

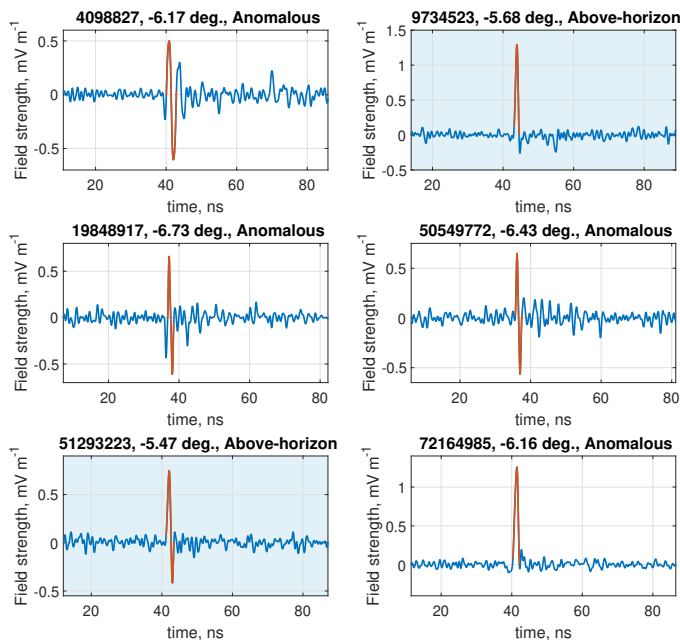


FIG. 4: The incident field strength vs. time for the six near-horizon events, all of which have the same (non-inverted) polarity: two above-horizon (pale blue background), and four below-horizon (white background) with anomalous polarity. These plots use the CLEAN deconvolution method as the waveform estimate.

For the same six events summarized in Table I, Fig. 4 shows the CLEAN deconvolutions scaled to give their incident electric field strength at the ANITA payload. Here the subdominant Vpol waveform component was added coherently to the Hpol component to produce the best estimate of the intrinsic

field strength of the incident pulse in the plane of polarization. Calibration and deconvolution systematic errors on the field strength are estimated to be $\sim 30\%$. The region of the pulses which are used to determine polarity are highlighted in red, and the background colors indicate events from above horizon (pale blue) or below horizon (white). The central segments of the waveforms annotated in orange show the primary pole (for unipolar) or poles (for bipolar) that determine the polarity. In laboratory tests using known signals plus thermal noise, CLEAN gave the most consistent recovery of the intrinsic waveform in the presence of noise, and thus we use the CLEAN waveform for the estimates in Fig. 4.

Event 4098827 had significant loss of bandwidth due to the three notch filters used to suppress electromagnetic interference for this event, and although the deconvolution is able to recover a portion of this signal via interpolation, the narrower effective bandwidth of this event is evident in the larger number of zero-crossings in the resulting waveform. Despite this, 4098827's polarity is in this case known with confidence, due to fortuitous observation of a normal three-notch-filter CR event [14] with a very similar waveform, and which had inverted polarity with respect to this event.

In addition to the dedicated CR analysis, a separate neutrino-focused analysis chain based only on the impulsive nature of events and spatial isolation of their locations also found the majority of the cosmic rays, separately confirming the efficacy of the CR methods [7]. This less rigorous analysis suggested possible associations with anthropogenic event clusters for two of the near-horizon CR; and for a third near-horizon CR, with a camp location that was free of any detectable anthropogenic interference [14]. Further study determined this result was due to imprecise event localization used in this analysis, and these associations were found to be unwarranted by the standards of the primary CR analysis.

In Table I, events 4098827 and 72164985 appear very near, but just below the horizon, by about 0.2° , about 1 and 2 standard deviations, respectively, for these two events. The standard error in angle given depends on their SNR, determined from ground-to-payload calibration pulsers during the flight. Both of these events may have a non-negligible statistical chance to be due to stratospheric CR, misidentified as below-

horizon events due to statistical fluctuations in the pointing reconstruction. To assess the chance of such a misidentification, we must consider the effects of grazing incidence RF propagation in the near-horizon atmosphere.

A detailed analysis of the effects of near-horizon propagation, including the use of GPS occultation data [21, 22], indicates that the refractivity gradient can lead to significant phase distortion if the ray paths fall within 1 km of the surface, a region that is comparable to the size of the first Fresnel zone for ANITA’s geometry [14]. Although we do not have direct measurements of the tropospheric parameters in the region that these events were observed, measurements taken at the South Pole indicate that spatial variations in the index of refraction observed in this near-surface atmosphere would lead to variations in the path delay across the wavefronts and loss of coherence at higher frequencies.

Such a loss of coherence does not appear consistent with our observations [14]. This suggests that if 4098827 and 72164985 arise from misidentified above-horizon CR, they may require an original above-horizon source direction that is $\gtrsim 0.1^\circ$ above the horizon to preserve the observed coherence of the events, reducing the chance that they are in fact due to pointing fluctuations.

In addition to these propagation considerations, we have also considered the effects of a residual unknown $\pm 0.1^\circ$ systematic pointing bias that might offset the apparent location of the events relative to their true direction. Evidence from our calibration and other data does not exclude possible bias at this level.

To estimate the overall significance of observing these four events given (1) the background estimate, (2) the chance for statistical polarity misidentification, and (3) the chance for misreconstruction of the event direction, we have used two independent statistical simulations, each of which vary parameters for all 27 CR with determined polarities, tabulating how often the outcomes randomly produce four or more such events in any combination. We allow variations for all types of systematic error noted above: a pointing bias, and a propagation restriction, and polarity misidentification, to provide conservative bounds on the significance.

Both simulations gave consistent results, indicating a p -value range of

$$3.7 \times 10^{-3} \geq p \geq 7.5 \times 10^{-5}$$

equivalent to between 2.7 - 3.8σ significance in Gaussian statistics [14]. While this confidence level is not adequate to conclude that these events may not be some combination of the different backgrounds, it is suggestive of a new class of CR-like events with Earth-skimming geometry.

ANITA-IV’s sensitivity exceeded that of any prior ANITA flight, and three of these four events are near the threshold of sensitivity, and thus would not have been observed previously. Currently, there is no radio air shower simulation that can treat events propagating in these very extreme conditions where it appears that a full-wave physical optics solution is necessary. Such full-wave simulations with scales that can

match the ANITA geometry are currently beyond the computing capabilities available for this work, and will require a follow-up investigation to understand ANITA’s acceptance to near-horizon air showers, and any relevant near-horizon propagation effects that may impact the significance of the observation.

While the significance of the data does not yet require it, we anticipate the question of a possible particle physics origin for these events. The four near-horizon events are not inconsistent with air showers initiated by τ -lepton decay after emergence of the τ from a charged-current neutrino event in the ice along the track direction. Because their track directions near tangential, the parent ν_τ would not suffer significant attenuation in the Earth, a problem that appeared to exclude a Standard-Model neutrino origin for the steeply-arriving anomalous events observed in earlier ANITA flights [23]. Further work is in progress to determine whether ANITA’s effective aperture for air showers generated by τ -lepton decay is consistent with possible ν_τ fluxes.

ANITA-IV was supported by NASA grant NNX15AC24G and related grants. We thank the staff of the Columbia Scientific Balloon Facility for their generous support. This work was supported by the Kavli Institute for Cosmological Physics at the University of Chicago. Computing resources were provided by the Research Computing Center at the University of Chicago and the Ohio Supercomputing Center at The Ohio State University. O. Banerjee and L. Cremonesi’s work was supported by collaborative visits funded by the Cosmology and Astroparticle Student and Postdoc Exchange Network (CASPEN). S. A. Wissel would like to thank the Cal Poly Frost Fund and the CSU Research, Scholarship, and Creative Activity (RSCA) Grant Program. The University College London group was also supported by the Leverhulme Trust. The National Taiwan University group is supported by Taiwan’s Ministry of Science and Technology (MOST) under its Vanguard Program 106-2119-M-002-011.

-
- [1] G. A. Askaryan, Excess Negative Charge of an Electron-Photon Shower And Its Coherent Radio Emission, *JETP* **14**, 441 (1962); also *JETP* **21**, 658 (1965).
 - [2] D. Saltzberg, *et al.* Observation of the Askaryan Effect: Coherent Microwave Cherenkov Emission from Charge Asymmetry in High-Energy Particle Cascades, *Phys. Rev. Lett.* **86** (2001) 2802.
 - [3] The ANITA Collaboration, P. W. Gorham, *et al.* [ANITA Collaboration], “Observations of the Askaryan Effect in Ice,” *Phys. Rev. Letters* **99**, 171101 (2007); arxiv.org/abs/hep-ex/0611008.
 - [4] The ANITA collaboration, Gorham, P. W. *et al.*, *Astropart. Phys.* **32**, 10-41 (2009).
 - [5] S. Hoover *et al.* [ANITA Collaboration], *Phys. Rev. Lett.* **105**, 151101 (2010).
 - [6] Constraints on the ultra-high energy cosmic neutrino flux from the fourth flight of ANITA, P. W. Gorham, *et al.* [ANITA collaboration], *Phys. Rev. D* **99**, 122001 (2019); [arXiv:1902.04005](https://arxiv.org/abs/1902.04005).
 - [7] Cao, Peng. University of Delaware, ProQuest Dissertations Pub-

- lishing, 2018. 13425957.
- [8] H. Schoorlemmer, *et al.*, [ANITA collaboration], “Energy and Flux Measurements of Ultra-High Energy CRs Observed During the First ANITA Flight” *Astropart. Phys.* 77, 32,(2016); also arXiv:1506.05396.
- [9] P. W. Gorham *et al.* [ANITA Collaboration], Characteristics of Four Upward-pointing Cosmic-ray-like Events Observed with ANITA, *Phys. Rev. Lett.* (2016), 117, 071101, arxiv.org/abs/1603.05218
- [10] P. Allison *et al.* [ANITA Collaboration], “Constraints on the diffuse high-energy neutrino flux from the third flight of ANITA,” *Phys. Rev. D* 98, 022001 (2018); arxiv.org/abs/1803.02719.
- [11] P. Gorham, *et al.* [ANITA Collaboration], “Observation of an Unusual Upward-going Cosmic-ray-like Event in the Third Flight of ANITA,” *Phys. Rev. Lett.* 121, 161102 (2018); arxiv.org/abs/1803.05088.
- [12] Coherent Transition Radiation from the Geomagnetically Induced Current in Cosmic-Ray Air Showers: Implications for the Anomalous Events Observed by ANITA, Krijn D. de Vries and Steven Prohira *Phys. Rev. Lett.* 123, 091102
- [13] Shoemaker, I., Kusenko, A., Kuipers Munneke, P., Romero-Wolf, A., Schroeder, D., & Siebert, M. (2020). Reflections on the anomalous ANITA events: The Antarctic subsurface as a possible explanation. *Annals of Glaciology*, 1-7. doi:10.1017/aog.2020.19
- [14] See Supplemental material at [URL to be inserted by publisher] describing the more specialized details of these analysis.
- [15] Wiener, Norbert (1949). *Extrapolation, Interpolation, and Smoothing of Stationary Time Series*. New York: Wiley. ISBN 978-0-262-73005-1.
- [16] H. Ogbom, J. (1974), “Aperture synthesis with a non-regular distribution of interferometer baselines”, *Astrophys. J. Suppl. Ser.*, 15, 417-426.
- [17] Han Deng, J. Li, L. Yang and T. Talty, “Intra-vehicle UWB MIMO channel capacity,” 2012 IEEE Wireless Communications and Networking Conference Workshops (WCNCW), Paris, 2012, pp. 393-397, doi: 10.1109/WCNCW.2012.6215529.
- [18] A. Chandra et al., “Serial subtractive deconvolution algorithms for time-domain ultra wide band in-vehicle channel sounding,” in *IET Intelligent Transport Systems*, vol. 9, no. 9, pp. 870-880, 11 2015, doi: 10.1049/iet-its.2014.0287.
- [19] R. Neelamani, Hyeokho Choi and R. Baraniuk, “ForWaRD: Fourier-wavelet regularized deconvolution for ill-conditioned systems,” in *IEEE Transactions on Signal Processing*, vol. 52, no. 2, pp. 418-433, Feb. 2004, doi: 10.1109/TSP.2003.821103.
- [20] D. Bhattacharya, 2019, unpublished PhD dissertation, George Washington University.
- [21] A technical description of atmospheric sounding by GPS occultation, G.A. Hajj, E.R. Kursinski, L.J. Romans, W.I. Bertiger, S.S. Leroy, *Journal of Atmospheric and Solar-Terrestrial Physics* 64 (2002) 451-469.
- [22] Josep M. Aparicio¹, Estel Cardellach, and Hilda Rodriguez, Information content in reflected signals during GPS Radio Occultation observation, *Atmos. Meas. Tech.*, 11, 1883-1900, 2018.
- [23] A. Romero-Wolf *et al.* [ANITA collaboration], Comprehensive analysis of anomalous ANITA events disfavors a diffuse tau-neutrino flux origin, *Phys. Rev. D* 99, 063011 (2019); DOI: 10.1103/PhysRevD.99.063011